pH-sensitive polymer-modified liposome-based immunity-inducing system : effects of inclusion of cationic lipid and CpG-DNA

pH-sensitive polymer-modified liposome-based immunity-inducing system: effects of inclusion of cationic lipid and CpG-DNA

Yuta Yoshizaki[1], Eiji Yuba[1,*], Naoki Sakaguchi[2], Kazunori Koiwai[2], Atsushi Harada[1], and Kenji Kono[1]

[1]Department of Applied Chemistry, Graduate School of Engineering, Osaka Prefecture University, 1–1 Gakuen–cho, Naka–ku, Sakai, Osaka 599–8531, Japan

[2]Terumo Corp., Ashigarakami–gun, Kanagawa 259–0151, Japan

***Corresponding author: Eiji Yuba**

Department of Applied Chemistry, Graduate School of Engineering,

Osaka Prefecture University, 1-1 Gakuen-cho, Naka-ku, Sakai, Osaka 599-8531, Japan

Tel: +81-722-54-9913; Fax: +81-722-54-9913; yuba@chem.osakafu-u.ac.jp

Keywords: pH–sensitive liposome / adjuvant / cationic lipid / CpG-DNA / cancer immunotherapy / dendritic cell

Abstract

Efficient vaccine carriers for cancer immunotherapy require two functions: antigen delivery to dendritic cells (DCs) and the activation of DCs, a so-called adjuvant effect. We previously reported antigen delivery system using liposomes modified with pH-sensitive polymers, such as 3-methylglutarylated hyperbranched poly(glycidol) (MGlu-HPG), for the induction of antigen-specific immune responses. We reported that inclusion of cationic lipids to MGlu-HPG-modified liposomes activates DCs and enhances antitumor effects. In this study, CpG-DNA, a ligand to Toll-like receptor 9 (TLR9) expressing in endosomes of DCs, was introduced to MGlu-HPG-modified liposomes containing cationic lipids using two complexation methods (Pre-mix and Post-mix) for additional activation of antigen-specific immunity. For Pre-mix, thin membrane of lipids and polymers were dispersed by a mixture of antigen/CpG-DNA. For Post-mix, CpG-DNA was added to pre-formed liposomes. Both Pre-mix and Post-mix delivered CpG-DNA to DC endosomes, where TLR9 is expressing, more efficiently than free CpG-DNA solution did. These liposomes promoted cytokine production from DCs and the expression of co-stimulatory molecules *in vitro* and induced antigen-specific immune responses *in vivo*. Both Pre-mix and Post-mix exhibited strong antitumor effects compared with conventional pH-sensitive

polymer-modified liposomes. Results show that inclusion of multiple adjuvant molecules into pH-sensitive polymer-modified liposomes and suitable CpG-DNA complexation methods are important to design potent vaccine carriers.

1. Introduction

Recent advances in immunology and biotechnology have produced efficient therapeutic approaches based on human immune systems. Especially because of the success of immune checkpoint inhibitors such as ipilimumab and nivolumab, cancer immunotherapy is nearly regarded as a fourth standard cancer therapy [1]. Immune checkpoint inhibitors have revealed clearly that immune systems can attack and eliminate cancer cells, with roles played mainly by cytotoxic T lymphocytes (CTLs). Establishing more effective cancer immunotherapy requires an effective CTL induction system and canceling of immunosuppressive effects in tumor microenvironments using immune checkpoint inhibitors. Adoptive T cell transfer therapy, which is the treatment by administration of cancer-specific T cells cultured *ex vivo*, has been studied for such purposes [2]. Another strategy for the induction of cancer-specific CTLs is the utilization of dendritic cells (DCs). DCs can induce cancer-specific CTLs *via* presentation of the endogenous antigen mediated by major histocompatibility complex (MHC) class I molecules [3]. In general, exogenous antigen is presented by MHC class II to induce helper T lymphocytes (Th), which assist the CTL-mediated cellular immune responses or B cell-mediated antibody production. Therefore, the delivery of exogenous antigen into cytosol is necessary to regard the antigen as an endogenous antigen and to

induce MHC class-I-mediated antigen presentation. Therefore, the cytoplasmic delivery system of exogenous antigen to DCs is necessary to induce antigen-specific CTLs for the establishment of efficient cancer immunotherapy.

Cytoplasmic delivery systems of various types have been reported in the literature [4]. Among them, lipid-based antigen delivery carriers are particularly useful because they can induce membrane fusion or destabilization of endosomal membrane and can achieve cytoplasmic delivery of antigen. Typical examples of cytoplasmic delivery systems using lipid-based carrier are viral fusogenic protein-incorporated liposomes such as Sendai virus-derived fusogenic protein-introduced liposomes [5] or Virosome, influenza virus fusogenic protein (hemagglutinin)-incorporated liposomes [6]. Sendai virus-derived fusogenic protein-introduced liposomes generated fusion with plasma membrane and directly delivered the antigenic protein into cytosol of DCs [7]. Virosome induces fusion with endosomal membrane because hemagglutinin changes its conformation under weakly acidic pH in endosomes. Also, exposed hydrophobic moiety in hemagglutinin is inserted to the endosomal membrane, thereby causing the adjacency of virosome to the endosomal membrane. Sendai virus-derived fusogenic protein-introduced liposomes and Virosome could induce antigen-specific CTLs but they might induce unexpected immunity-related effects derived from viral components.

Therefore, cytoplasmic delivery systems without viral components are sought, such as liposomes modified with synthetic molecules or peptides having fusogenic activity. We previously reported synthetic fusogenic polymers using carboxylated poly(glycidol) derivatives and these polymer-modified liposomes for the cytoplasmic delivery of contents [8–12]. Carboxylated poly(glycidol) derivatives change their properties from hydrophilic to hydrophobic after protonation of carboxylic acid groups under weakly acidic pH and destabilize lipid membrane. Modification of egg yolk phosphatidylcholine (EYPC) liposomes with these polymers produces liposomes having pH-responsive fusogenic ability [8]. Especially, 3-methylglutarylated hyperbranched poly(glycidol) (MGlu-HPG, Fig. 1) showed excellent membrane disruptive ability under acidic pH because of its bulky three-dimensional structures [8]. MGlu-HPG-modified liposomes delivered ovalbumin (OVA) or its CTL epitope peptide used as model antigens to cytosol of DCs and induced stronger OVA-specific CTL responses than complete Freund's adjuvant [8-10].

In the antigen presentation process, DCs present antigen to T cells *via* MHC molecules (first signal), activate T cells by co-stimulatory molecules (second signal), and cytokines (third signal) [13, 14]. These signals are important for the induction of antigen-specific immune response. If antigen presentation occurs without the second

signal, then immune tolerance (anergy of T cells) is induced [15]. Furthermore, cytokines play crucially important roles of controlling immunity and deciding the T cell subtype [16]. Activated state (matured) DCs express high levels of MHC molecules and co-stimulatory molecules; moreover, they produce specific cytokines [17]. Therefore, efficient antigen carriers require not only cytoplasmic delivery performance but also activation ability of DCs to induce DC maturation, which is designated as an adjuvant function.

Adjuvant function is crucially important for vaccines to control immune response through DC activation [18]. Alum has been the most famous and general adjuvant since the 1920s. A vaccine composed of antigen and alum can induce antigen-specific antibody response [19]. However, because alum has no ability to induce CTL response [19] and administration of alum/OVA mixture to tumor-bearing mice showed no antitumor effect in our experimental condition (data not shown). Therefore, more efficient adjuvant molecules are necessary to activate CTL response. Reportedly, surface chemistry of nanoparticles strongly affected their adjuvant function. For examples, cationic polysaccharide (chitosan)- or hydrophobic pluronic F68-coated lipid nanoparticles activated peripheral blood mononuclear cells [20]. Carboxylated graphene oxides or poly(ethylene imine)-modified graphene oxides showed activation of APCs,

whereas poly(ethylene glycol) (PEG)-modified ones were inert to immune systems [21]. Ma et al also reported the importance of terminal functional groups of PEG on quantum dots for activation of APCs [22]. Cationic lipids and cationic lipid-introduced liposomes also have adjuvant functions [23, 24]. We recently reported that the incorporation of 3, 5-didodecyloxybenzamidine (TRX, Fig. 1) as a cationic lipid to MGlu-HPG-modified liposomes promoted their activation property of DC by the synergetic effect of carboxyl groups on MGlu-HPG and cationic functional groups of TRX [25]. As a result, TRX-inclusion increased the conjugation of MGlu-HPG polymers onto liposome surface *via* electrostatic interaction with TRX and the increase of carboxylate density on liposome surface induced the activation of dendritic cells [25]. TRX-incorporated liposomes induced high CTL response and antitumor effect against tumor-bearing mice [25]. However, its therapeutic effect remained lower than that of liposomes containing monophosphoryl lipid A (MPLA), which is an adjuvant derived from bacterial lipopolysaccharide [25]. We examined the combination of TRX and MPLA for activation of antitumor immunity. Unexpectedly, inclusion of TRX and MPLA to MGlu-HPG-modified liposomes reduced the antitumor effect (unpublished data), which suggests the competition in intracellular signaling between TRX and MPLA.

Toll-like receptors (TLRs) are pattern recognition receptors (PRRs). DCs detect

and distinguish viruses and bacteria invading a living body using TLRs. Then they induce appropriate immunity against pathogens [26]. Many TLR ligands including MPLA, poly(I:C) and CpG-DNA have been explored as adjuvant molecules for antigen delivery system. Among them, we focused on CpG-DNA because CpG-DNA is unmethylated CG sequence-containing oligonucleotide and can be chemically synthesized in a low cost. Actually, CpG-DNA has been used as adjuvant for activation of antigen-specific immune response by combination of various antigen delivery nanomaterials [27-30]. Because CpG-DNA is recognized by TLR9, which expresses in endosome of DCs [31], the delivery control of CpG-DNA molecules in DCs would be of importance to achieve efficient activation of DC *via* TLR9. Reportedly, TRX-introduced MGlu-HPG liposomes delivered their contents in endosomes rather than cytosol because of the restriction of MGlu-HPG polymers on the surface of liposomes [25]. In this study, CpG-DNA was introduced to pH-sensitive polymer (MGlu-HPG)-modified liposome-based antigen carrier to control intracellular distribution of CpG-DNA and improve their adjuvant function (Fig. 1). CpG-DNA has an anionic phosphoester backbone [32]. Therefore, CpG-DNA is expected to complex with cationic lipid (TRX) on the liposomal membrane through electrostatic interaction. In addition, multiple introduction of adjuvant molecules (CpG-DNA and TRX) is

expected to show synergistic effect on immunity induction. Here, two complexation methods of CpG-DNA to liposomes were investigated (Fig. 2): Pre-mix for which CpG-DNA was mixed with liposomal lipids when liposomes were formed and Post-mix for which CpG-DNA was mixed with pre-formed liposomes. The CpG-DNA complexation method effects on the immunity-inducing activity of liposomes were examined *in vitro* and *in vivo*.

2. Materials and Methods

2.1. Materials

EYPC was kindly donated by NOF Co. (Tokyo, Japan). 3, 5–Didodecyloxybenzamidine hydrochloride (TRX) were kindly donated by Terumo Corp., Ltd. (Kanagawa, Japan). Lissamine rhodamine B–sulfonyl phosphatidylethanolamine (Rh–PE) was purchased from Avanti Polar Lipids (Birmingham, AL, USA). OVA, bovine serum albumin (BSA) and MPLA were purchased from Sigma (St. Louis, MO.). Triton X–100 were obtained from Tokyo Chemical Industries Ltd. (Tokyo, Japan). Quant-iT Oligreen ssDNA reagent was obtained from Molecular Probes (Oregon, USA). ODN 1826 (CpG-DNA: 5'-TCCATGACGTTCCTGACGTT-3') and Tween20 were obtained from Nacalai Tesque, Inc., (Kyoto, Japan). 3‐Methylglutarylated

hyperbranched poly(glycidol) with polymerization degree of 60 (MGlu‐HPG) was prepared as previously reported [8]. The ratios of hydroxyl units, MGlu units and decyl amide units for MGlu‐HPG was 9/80/11, as estimated using ^{1}H NMR [8].

2.2. Cell culture

DC2.4 cells, which were an immature murine DC line, were provided from Dr. K. L. Rock (Harvard Medical School, USA) and were grown in RPMI–1640 (Nacalai Tesque) supplemented with 10% FBS (MP Biomedical, Inc.), 2 mM L–glutamine (Wako), 100 mM MEM nonessential amino acid (Nacalai Tesque), 50 μM 2–mercaptoethanol (2–ME, Gibco), 100 U/mL penicillin, and 100 μg/mL streptomycin at 37 °C [33]. E.G7–OVA, which is a chicken egg OVA gene–transfected murine T lymphoma and which presents OVA with MHC class I molecules, was obtained from the American Type Culture Collection (Manassas, VA) [34].

2.3. Animals

Female C57BL/6 mice (H–2^{b}, 7 weeks old) were purchased from Oriental Yeast Co., Ltd. (Tokyo, Japan). The experiments were carried out in accordance with the guidelines for animal experimentation in Osaka Prefecture University.

2.4. Preparation of liposomes

Liposomes were prepared according to the standard thin film hydration method.

To a dry, thin membrane of EYPC and TRX (0 or 30 mol%) (total lipids; 1.25×10^{-5} mol) and MGlu–HPG (lipids/polymer = 7/3, w/w) was added 500 μL of OVA (4 mg/mL) phosphate buffered saline (PBS) (pH 7.4) and the mixture was sonicated for 2 min using a bath–type sonicator. The liposome suspension was further hydrated by freezing and thawing, and was extruded through a polycarbonate membrane with a pore size of 100 nm. The liposome suspension was centrifuged with the speed of 55,000 rpm for 2 h at 4 °C twice to remove free OVA and CpG-DNA. For CpG-DNA inclusion to liposomes, two complexation methods were examined. In the case of Pre-mix, mixed thin membrane was dispersed by mixture of OVA/CpG-DNA (2.5, 5, 7.5 g/mol lipid) in PBS. Lipid concentration and OVA encapsulation were determined by Test-Wako C (Wako Pure Chemical Industries, Ltd) and Coomassie (Bradford) Protein assay reagent (Thermo-Scientific). CpG-DNA amounts in liposomes were determined by Quant-iT Oligreen ssDNA assay as following procedure. Lipid dispersion was mixed with Triton-X 100 (0.2% vol) and Oligreen ssDNA assay reagent in fluorescence microtiter plate. Microplate was excited at 480 nm and fluorescence emission intensity was detected at 520 nm using Microplate Reader (SH-8000 CORONA ELECTRIC Co., Ltd.).

2.5. Dynamic light scattering and zeta potential

Diameters and zeta potentials of the liposomes (0.1 mM lipids) in 0.1 mM phosphate aqueous solution were measured using a Zetasizer Nano ZS ZEN3600 (Malvern Instruments Ltd, Worcestershire, UK). Data was obtained as an average of more than three measurements on different samples.

2.6. Cellular uptake of liposome and CpG-DNA

The DC2.4 cells (1×10^5 cells) cultured for 2 days in a 12-well plate were washed with Hank's balanced salt solution (HBSS) and then incubated in culture medium. The liposomes which lipids were substituted by Rh-PE (0.6 mol%) or the liposomes containing FITC-CpG-DNA were added gently to the cells and incubated for 4 h at 37 °C. The cells were washed with HBSS three times, and then the detached cells using trypsin were applied to a flow cytometer (CytoFlex, Beckman Coulter, Inc).

2.7. Intracellular behavior of liposomes

The FITC‐CpG-DNA‐incorporated liposomes containing Rh‐PE were prepared as described above except that a mixture of polymer and lipids containing Rh‐PE (0.6 mol%) was dispersed in PBS containing FITC‐CpG-DNA (5 g/mol lipid). DC2.4 cells (2×10^5 cells) cultured 2 days in 35–mm glass–bottom dishes were washed with HBSS, and then incubated in serum–free RPMI–1640 medium (1 mL). The FITC–CpG-DNA‐loaded liposomes (0.1 mM of lipid concentration, 5 g/mol lipid of

CpG-DNA concentration, total volume was 2 mL) were added gently to the cells and incubated for 4 h at 37 °C. After the incubation, the cells were washed with HBSS three times. In the case of staining cellular acidic compartments, LysoTracker Red or LysoTracker Green (Invitrogen) was used. Confocal laser scanning microscopic (CLSM) observation of these cells was performed using LSM 5 EXCITER (Carl Zeiss Co. Ltd.). Co-localization analysis was performed with LSM Software ZEN 2009 (Carl Zeiss Co. Ltd.).

2.8. Cytokine production from DC2.4 cells treated with liposomes

The DC2.4 cells (3×10^5 cells) cultured for 2 days in a 6-well plate were washed with HBSS, and then incubated in serum–free RPMI–1640 medium (2 mL).Cytokine (TNF–α and IL–12) production in supernatants of DC2.4 cells treated with liposomes was measured using an enzyme-linked immunosorbent assay kit (ELISA Development Kit, PeproTech EC Ltd.) according to the manufacture's instruction.

2.9. Analysis of liposome-treated DC phenotype

The DC2.4 cells (3×10^5 cells) cultured for 2 days in a 6-well plate were washed with HBSS, and then incubated in serum–free RPMI–1640 medium (2 mL). The OVA-loaded liposomes (0.1 mM of lipid and 1 μg/mL CpG-DNA concentration, 1 mL)

were added gently to the cells and incubated for 6 h at 37 °C. The cells were washed with HBSS three times and cultured for 20 h. Cell phenotype was confirmed by a flow cytometric analysis. Briefly, 10^6 cells in 100 μL of staining buffer (PBS containing 0.1% BSA and 0.01% sodium azide) were incubated for 30 min on ice with the anti–Fc γRII/III monoclonal antibody (eBioscience, 2.4G2) to block nonspecific binding of the subsequently used antibody reagents. The cells were re–suspended in 100 μL of staining buffer and incubated for 30 min on ice, using the manufacturer's recommended amounts of biotinylated antibodies: anti–mouse H–$2K^b$/D^b (BD Pharmingen, 28–8–6) and FITC–labeled anti–CD80 (abcam, 16–10A1). The cells were then re–suspended in 100 μL of staining buffer containing 10 μL of R‑Phycoerythrin (PE)–conjugated streptavidin (Sigma), and relative fluorescence intensity was measured against cells treated with PE–conjugated streptavidin alone. After incubation for 30 min on ice, 10,000 events of the stained cells were analyzed for surface phenotype, using a flow cytometer (CytoFlex, Beckman Coulter, Inc). Between all incubation steps, cells were washed three times with staining buffer.

2.10. *In vivo* stimulation of antigen-specific T cells

50 μg of OVA‑loaded liposomes or PBS were subcutaneously injected into the right backs of the mice under anesthesia twice at a week intervals. After a week from

second immunization mice were sacrificed and splenocytes were suspended in RPMI–1640 medium supplemented with 10% FBS, 100 U/mL penicillin, 100 μg/mL streptomycin, 50 μM 2–ME. Splenocytes (2×10^6 in 2 mL) were cultured with or without 50 μg/mL of OVA for 5 days. After incubation, the concentration of IFN‑γ was measured using murine IFN‑γ ELISA development kit (PeproTech, London, UK) according to the manufacture's instruction.

2.11. Treatment of tumor‑bearing mice with liposomes

E.G7–OVA cells (1×10^6 cells) were subcutaneously inoculated into the left backs of C57BL/6 mice under anesthesia with isoflurane. On days 5 and 12, 50 μg of OVA‑loaded liposomes were subcutaneously injected into the right backs of the mice under anesthesia with isoflurane. Tumor sizes were monitored from the day of inoculation. Mice immunized with PBS were used as controls to confirm the development of cancer following the first inoculation with E.G7–OVA cells. Mice were sacrificed when tumor volumes become over 2,500 mm^3. All treated groups contained four mice.

2.12. Statistical analysis

Student's *t*–test (Fig. 3) or Tukey-Kramer-test were performed in the statistical evaluation of the results (Figs. 4, 6-8). Survival data in Figure 9 was evaluated using

Log-rank test (Tables S2-S4).

3. Results and Discussion

3.1. Preparation of cationic lipid- and CpG-DNA-introduced liposomes

This study investigated the inclusion of both cationic lipids and CpG-DNA to pH-sensitive polymer-modified liposomes for the preparation of an efficient antigen delivery system. Figure 2 presents a summary of the preparation scheme of antigen-loaded liposomes used for this study. A mixed thin membrane composed of EYPC and MGlu-HPG was dispersed in PBS containing OVA. Liposome suspension was extruded through a 100 nm polycarbonate membrane. Then it was purified by ultracentrifugation. This liposome was designated as Lip. TRX-Lip was prepared from mixed thin membrane composed of EYPC, TRX, and MGlu-HPG according to the same procedure. Two complexation methods of CpG-DNA were examined: Pre-mix for which a mixed thin membrane with or without TRX was dispersed in a mixture of OVA/CpG-DNA solution, designated respectively as Pre-mix TRX+ and Pre-mix TRX–. The CpG-DNA contents in liposomes were ascertained using an ssDNA assay kit (Fig. 3). Figure 3 shows that the CpG-DNA contents in Pre-mix TRX+ were significantly greater than those of Pre-mix TRX–. More than 80% of CpG-DNA in feed complexed

with TRX-containing liposomes, whereas the complex efficiency of Pre-mix TRX– was less than 13%. These results demonstrate that CpG-DNA binds efficiently to cationic lipids on the liposomal membrane *via* electrostatic interaction. In addition, the stability of CpG-DNA loading was evaluated using Pre-mix TRX+. After 24 h-incubation in a physiological condition, Pre-mix TRX+ suspension was ultracentrifuged and CpG-DNA concentrations in liposome pellet and supernatant were respectively determined using ssDNA assay kit. According to the results, only 3.7 ± 1.3 % of CpG-DNA was detected from supernatant (n = 3). This indicates that more than 96% of CpG-DNA molecules tightly bound to liposome surface *via* electrostatic interactions with TRX even after 24 h-incubation. Another method for CpG-DNA complexation is Post-mix for which the same amount of CpG-DNA in Pre-mix TRX+ was added to pre-formed Lip and TRX-Lip, which are designated respectively as Post-mix TRX– and Post-mix TRX+. Because they were used without further purification, the content of CpG-DNA (4.60 ± 0.44 g/mol, determined by ssDNA assay kit) was almost same with feed content (5 g/mol). OVA content of each liposome was summarized in Table S1. TRX-inclusion increased the OVA content per liposome (from 150 g/mol to 240 g/mol), which might result from electrostatic interaction between TRX and acidic protein OVA. In contrast, CpG-DNA inclusion hardly affected the OVA contents in liposomes.

The particle size and ζ-potential of each liposome at pH 7.4 were evaluated using DLS and electrophoretic light scattering (Table 1). All liposomes were approximately 100 nm, which corresponds to the pore size of the polycarbonate membrane used for extrusion. All liposomes showed negative values of zeta potentials, which indicates that the liposome surface was covered by MGlu-HPG having many carboxyl groups. The TRX-containing liposomes exhibited more negative zeta potentials than liposomes without TRX, which suggests that the introduction of cationic lipid increased the amounts of MGlu-HPG polymers on the surface of liposome *via* electrostatic interactions. That result is consistent with those presented in earlier reports of the literature [25]. The inclusion of CpG-DNA to liposomes only slightly affected the size and zeta potentials of each liposome without CpG-DNA. Therefore, liposomes might retain their structure even in the presence of CpG-DNA molecules.

3.2. Cellular association of cationic lipid- and CpG-DNA-introduced liposomes

Next, the cellular association of liposomes to dendritic cells was examined. For 4 h, DC2.4 cells were treated with rhodamine lipid-incorporated liposomes. Then, cellular fluorescence was measured using flow cytometric analysis. Figure 4A shows that liposomes with TRX (TRX-Lip, Pre-mix TRX+) exhibited over 10 times higher

cellular fluorescence than those of liposomes without TRX (Lip, Pre-mix TRX–). Reportedly, more anionic nanoparticles are taken up more efficiently by dendritic cells or macrophages by the recognition of scavenger receptors on these cells, which are receptors to recognize anionic surface of apoptotic cells or aged erythrocytes [35, 36]. Liposomes with TRX showed much lower zeta potentials than those of liposomes without TRX (Table 1). Therefore, liposomes with TRX might be recognized efficiently by scavenger receptors on DC2.4 cells, which is consistent with results of our earlier study [25]. The inclusion of CpG-DNA to Lip or TRX-Lip caused the reduction of cellular association of liposomes to some extent, which suggests that CpG-DNA on the liposome surface might interrupt the interaction of carboxylate of MGlu-HPG with scavenger receptors.

Cellular association of CpG-DNA was investigated using FITC-labeled CpG-DNA (Fig. 4B). Compared with free CpG-DNA solution, Pre-mix TRX+ showed much higher FITC fluorescence, indicating that CpG-DNA was delivered efficiently by Pre-mixed liposomes. In contrast, both Post-mix TRX–/+ showed lower fluorescence intensity than that of free CpG-DNA, which suggests that the liposomes with negative charges (Table 1) might act as an inhibitor and suppress the cellular association of CpG-DNA molecules.

3.3. Intracellular distribution of cationic lipid- and CpG-DNA-introduced liposomes

TLR9 exists at endosomal lumen of immunocompetent cells. Therefore, precise delivery of CpG-DNA molecules to the inside of endosomes might cause efficient activation of immunocompetent cells. Therefore, the intracellular distribution of CpG-DNA delivered by liposomes was investigated next. For 4 h, DC2.4 cells were treated with FITC-CpG-DNA solution or FITC-CpG-DNA-introduced liposomes. The DC2.4 cells were then observed using CLSM (Fig. 5A). For cells treated with CpG-DNA solution, most of the FITC fluorescence was observed from the cell periphery, which suggests that most of the CpG-DNA adsorbed onto the cell surface and that their internalization efficiency was quite low. For cells treated with Pre-mix TRX–, red punctate fluorescence and green fluorescence were observed from the same intracellular locations, indicating that liposomes and CpG-DNA were internalized to cells. However, their fluorescence was quite low because the cellular association of liposomes and CpG-DNA contents in liposomes were low (Figs. 3 and 4A). In contrast, cells treated with Pre-mix TRX+ showed much stronger red and green fluorescence than those of Pre-mix TRX-. According to the co-localization analysis of FITC fluorescence

derived from CpG-DNA and rhodamine fluorescence derived from liposome, over 80% of FITC pixels in the region of interest (ROI, dashed white lines in the CLSM image) co-localized with rhodamine pixels (Fig. 5B), which indicates that Pre-mix TRX+ efficiently delivered both liposome and CpG-DNA to inside of cells. For more detailed evaluation of intracellular distribution of liposomes and CpG-DNA, cells treated with Pre-mix TRX+ were stained with LysoTracker (Fig. 5C). Figure 5C demonstrates that rhodamine and FITC-CpG-DNA fluorescence derived from Pre-mix TRX+ overlapped respectively with LysoTracker green and LysoTracker red. Their co-localization efficiency in the ROI was higher than 80% (Fig. 5D). These results suggest that Pre-mix TRX+ delivered CpG-DNA to endosomes in DC2.4 cells. Therefore, Pre-mix TRX+ is expected to stimulate DCs effectively *via* interaction with TLR9.

Intracellular delivery performance of CpG-DNA by "Post-mix" liposomes was also examined (Fig. 5A). In the case of cells treated with Post-mix TRX–, red fluorescence was located within cells, but most of the green fluorescence was observed from the cell periphery as it was in the case of free CpG-DNA solution-treated cells. This result suggests that liposomes and CpG-DNA were taken up independently by cells in the case of Post-mix TRX–. It is particularly interesting that in the case of cells treated with Post-mix TRX+, most of the green fluorescence located within cells, unlike

the case of Post-mix TRX–. To elucidate the internalization mechanism of CpG-DNA by Post-mix TRX+, time-dependence of the intracellular distribution of CpG-DNA and liposomes was evaluated (Fig. S1). Figure S1 shows that green and red fluorescence was observed only slightly at an earlier stage (30 min of incubation time). After 1-h incubation, strong red fluorescence was observed from inside of cells. Moreover, the green fluorescence almost overlapped with the red fluorescence. After 4-h incubation, both red and green fluorescence were observed from inside the cells, but a part of the green fluorescence was located at a different site from that of red fluorescence. These results suggest that CpG-DNA might form a complex with liposomes in the culture medium and be internalized. Eventually, it is released from liposomes. To investigate the complex formation with CpG-DNA and liposomes, Lip or TRX-Lip and CpG-DNA were incubated for 10 min or 4 h and ultracentrifuged. Then the amounts of CpG-DNA in the supernatant and the precipitated liposomes were measured using an ssDNA assay kit (Fig. S2). According to Figure S2, about 60% of CpG-DNA was detected from the liposome fraction after 4 h-incubation with TRX-Lip, whereas almost all CpG-DNA molecules were detected from the supernatant in the case of Lip. These results indicate that CpG-DNA can bind to TRX-Lip *via* electrostatic interaction in Post-mix TRX+. After application to culture medium, some CpG-DNA molecules might start to bind to

TRX-Lip. Then, CpG-DNA/TRX-Lip complexes might internalize to cells. Therefore, Post-mix TRX+ can promote the internalization of CpG-DNA to dendritic cells. The co-localization efficiency of FITC with rhodamine was also evaluated between Pre-mix TRX+ and Post-mix TRX+ (Fig. 5B). Figure 5A shows that the ROI was set only to the inside of cells, as shown by dashed white lines in the CLSM images. Pre-mix TRX+ showed higher than 80% co-localization efficiency, as described above. In contrast, Post-mix TRX+ exhibited low co-localization efficiency compared with Pre-mix TRX+. MGlu-HPG-modified liposomes with TRX (TRX-Lip) are destabilized in response to weakly acidic pH inside of endosomes, as described in reports of earlier studies [25]. However, because CpG-DNA molecules in Pre-mix TRX+ might bind tightly to liposomal membrane *via* electrostatic interaction, CpG-DNA molecules might exist in endosomes with liposomes even after pH-responsive destabilization of liposomes. In contrast, the interaction between CpG-DNA and liposomes in Post-mix TRX+ might be low. Therefore, CpG-DNA molecules were released from endosomes when the endosomal membrane was destabilized by TRX-Lip. Such differences in the intracellular distribution of CpG-DNA inside of dendritic cells might cause the different activation profiles of dendritic cells, as described below.

3.4. Activation of dendritic cells by cationic lipid- and CpG-DNA-introduced liposomes

Next, the activation of dendritic cells by liposomes was evaluated in the viewpoints of cytokine production from DCs or upregulation of surface marker molecules. Figure 6 depicts the cytokine production from DC2.4 cells treated with CpG-DNA or various liposomes. Compared with cells with no treatment, cells treated with CpG-DNA solution produced high levels of TNF-α, which indicates that DC2.4 cells were activated by CpG-DNA, but no production of IL-12 was observed. Lip-treated cells also produced TNF-α, but various amounts of CpG-DNA inclusion to Lip by Pre-mix method (Pre-mix TRX–) did not affect the TNF-α production from cells. In addition, IL-12 production was not detected by these liposomes under experimental conditions. Compared with Lip and Pre-mix TRX–, TRX-Lip induced high levels of both TNF-α and IL-12 production, which is consistent with results of our earlier study [25]. Furthermore, inclusion of CpG-DNA to TRX-Lip by Pre-mix method strongly promoted TNF-α and IL-12 production but not by Post-mix method. Considering the difference in intracellular distribution of CpG-DNA between Pre-mix TRX+ and Post-mix TRX+ (Fig. 5A), Pre-mix TRX+, which mainly delivered CpG-DNA to endosomes, might induce the activation of cells through TLR9 in endosomes more

efficiently than Post-mix TRX+, which delivered CpG-DNA not only to endosomes but also to cytosol (Figs. 5A and S1), resulting in higher production of cytokines. IL-12 from DCs is the determinant factors of the differentiation of naive Th into Th1 [37]. Therefore, Pre-mix TRX+ is expected to promote cellular immune response through Th1 induction.

Surface marker molecules such as MHC classes I, II, and co-stimulatory molecules (CD80) play important roles in antigen presentation. Maturated DCs highly express MHC and co-stimulatory molecules and lead the activation of antigen-specific immune responses. Therefore, the expression of these surface markers on DC2.4 cells treated with CpG-DNA or various liposomes was analyzed using immunofluorescence staining (Figs. 7 and S3). The treatment of CpG-DNA solution affected the expression of MHC and CD80 molecules only slightly. Cells treated with Lip showed a slight increase of MHC class I molecules but not of CD80 molecules, which indicates that MGlu-HPG liposomes with no adjuvants (Lip) were unable to activate the dendritic cells fully. Compared with Lip, TRX-Lip promoted the expression of both MHC and CD80 molecules. This result indicates that TRX induced maturation of DCs, as reported previously [25]. CpG-DNA-introduced liposomes (Pre-mix TRX+ and Post-mix TRX+) also induced strong maturation of DC2.4 cells, but no significant difference exists

between TRX-Lip, Pre-mix, and Post-mix, except for CD80 expression. Figure 7C shows that Post-mix showed high expression of CD80 compared with Pre-mix. As shown in Fig. S1, CpG-DNA molecules in Post-mix TRX+ first bound to liposomes. Then they were delivered not only to endosomes but also to cytosol. The cytosol contains inflammasome of NALP3, which is known as a cytosolic DNA sensor [38]. Therefore, Post-mix TRX+ might activate dendritic cells not only by TLR9 in endosome but also NALP3 in cytosol. Such multiple stimulations might induce the high expression of CD80 molecules by Post-mix TRX+. Therefore, it is likely that methods of CpG-DNA inclusion to liposomes (Pre-mix or Post-mix) strongly affect the activation properties of dendritic cells, which might be attributed to the intracellular distribution of CpG-DNA.

3.5. *In vivo* immune responses of cationic lipid- and CpG-DNA-introduced liposomes

Next, *in vivo* immune response induced by liposomes was investigated. Various liposomes containing OVA were administered subcutaneously to mice. At 7 days after immunization, splenocytes were collected and cultured *in vitro* in the presence of OVA for 5 days. IFN-γ production from splenocytes during the 5-day culture was measured

using ELISA (Fig. 8). IFN-γ, which is known as Th1 cytokine, is important for induction and activation of cellular immunity. Splenocytes from mice treated with PBS only slightly produced IFN-γ irrespective to OVA concentration used *in vitro* culture. In contrast, in the cases of liposome-treated mice, IFN-γ production increased depending on OVA concentration during *in vitro* culture. These results indicate that OVA-specific cellular immune responses were induced in spleen by the administration of liposomes. According to the preliminary result of biodistribution of pH-sensitive polymer-modified liposomes after subcutaneous administration, most of liposomes remained at administered site even after 24 h and a part of liposome-derived fluorescence was overlapped with CD11c-expressing cells (dendritic cells) (data not shown). Considering the highly negative zeta potentials of liposomes (Table 1), the cellular association of liposomes to cells existing at administered site seems to be quite low except for antigen presenting cells (dendritic cells, Langerhans cells and macrophages), which have scavenger receptors to recognize the anionic molecules [35, 36]. Actually, cellular association of TRX-Lip to dendritic cells was quite high as previously reported [25]. Antigen presenting cells including CD11c-expressing dendritic cells that took up these anionic liposomes would migrate to lymph nodes. Actually, liposome-derived fluorescence was observed in lymph node (data not shown). Antigenic proteins were

released in endosomes and were delivered to cytosol of antigen presenting cells by membrane fusion activity of MGlu-HPG [25] and these cells were simultaneously activated by MGlu-HPG, TRX and/or CpG-DNA, which induced the antigen presentation to naïve T cells and subseqeunt activation of OVA-specific cellular immunity in spleen (Figure 9). Compared with Pre-mix TRX– and TRX-Lip, Pre-mix TRX+ and Post-mix TRX+ exhibited significantly strong cellular immune responses. This result suggests the importance of co-delivery of CpG-DNA and cationic lipids for induction of efficient cellular immune responses. Furthermore, Post-mix TRX+ induced the highest production level of IFN-γ unlike the *in vitro* results in cytokine production (Fig. 6). Considering the result in high expression of CD80 molecules by Post-mix TRX+ (Fig. 7C), high expression of co-stimulatory molecules might be the most important for induction of *in vivo* cellular immune responses.

3.6. Cancer immunotherapeutic effect by cationic lipid- and CpG-DNA-introduced liposomes

Therapeutic effects by liposomes on tumor-bearing mice were investigated. The E.G7-OVA cells, which are OVA-expressing tumor cells, were injected to mice. At 5 and 12 days after tumor inoculation, liposomes of various types were administered

subcutaneously to mice. Then, tumor growth was monitored. Figures 9A and 9B depict a comparison of the immunotherapeutic effects of TRX-Lip, Pre-mix TRX–, and Pre-mix TRX+. Compared with PBS-treated mice, all mice treated with these liposomes showed a decrease of tumor volumes, indicating that OVA-specific cellular immunity induced by these liposomes efficiently killed E.G7-OVA tumor cells. TRX-Lip and Pre-mix TRX– showed almost identical antitumor effects, which might be attributed to the almost identical cellular immune responses of these liposomes (Fig. 8). Among these liposomes, Pre-mix TRX+ exhibited the strongest antitumor effect and survival rate: the tumor volume of mice treated with Pre-mix TRX+ started to decrease 3 days after first immunization and disappeared once. Antitumor effect of conventional MPLA-introduced MGlu-HPG-modified liposomes was compared with Pre-mix TRX+ (Figure S4). MPLA-introduced MGlu-HPG-modified liposomes also showed strong antitumor effect but their survival was not significant with Pre-mix TRX+ ($p = 0.661$). Therefore, both TRX and CpG-DNA inclusion to MGlu-HPG-modified liposomes are effective to obtain adjuvant effect as same with conventional MPLA-introduced liposomes. Figures 9C and 9D compare the antitumor effects of Pre-mix TRX+ and Post-mix TRX+. As shown in Fig. 9C, Post-mix TRX+ showed tumor regression at earlier timing than that of Pre-mix TRX+ did, which might reflect higher cellular

immune response by Post-mix TRX+ (Fig. 8). However, survival of mice treated with Post-mix TRX+ was not significant compared with that of Pre-mix TRX+ ($p = 0.257$, Table S3). In these experiments, separate immunization of TRX-Lip and CpG-DNA solution at different sites was also examined as a comparison of Post-mix TRX+, which injects TRX-Lip and CpG-DNA solution at same sites immediately after mixing. Figures 9C and 9D both show that separate delivery of TRX-Lip and CpG-DNA produced relatively low antitumor effects and survival rates compared with those of Post-mix TRX+ ($p = 0.105$, Table S3). This result suggests that the co-delivery of antigen-loaded liposomes and adjuvants to DCs existing in same region is necessary for the induction of effective cellular immunity.

Finally, therapeutic effects for more progressive tumors were investigated (Figs. 9E and 9F). Liposomes were administered at Day 9 when tumor volumes reached approximately 500 cm^3, which is eight times larger than at Day 5. In these experiments, Lip, TRX-Lip, and Post-mix TRX+ were administered to tumor-bearing mice. Their therapeutic effects were evaluated. The tumor volumes of Lip-treated mice decreased to some degree, but increased again from Day 25. Both TRX-Lip and Post-mix TRX+ showed decreased tumor volume from earlier timing (Day 13) than Lip did (Day 20). In addition, Post-mix TRX+ showed stronger antitumor effects and prolongation of the

survival of mice than those of Lip did (p = 0.0311, Table S4). Therefore, the simultaneous delivery of CpG-DNA, cationic lipids and antigen by multiple adjuvants-introduced liposome-based systems is an effective strategy for induction of cancer-specific cellular immune responses.

4. Conclusion

This study investigated the immunity-inducing performance of CpG-DNA- and cationic lipid-introduced pH-sensitive polymer-modified liposomes. Two complexation methods of CpG-DNA to liposomes were compared: Pre-mix and Post-mix. Cationic lipid inclusion to liposomes promoted not only the binding of CpG-DNA to liposomes but also internalization of CpG-DNA. Both Pre-mix and Post-mix with cationic lipids activated dendritic cells efficiently *in vitro*. Especially, Post-mix promoted the expression of co-stimulatory molecules, which is important for efficient antigen presentation. Post-mix induced higher cellular immune responses than those of Pre-mix. Pre-mix and Post-mix showed almost identical antitumor effects on tumor-bearing mice and these therapeutic effects were high compared with conventional pH-sensitive polymer-modified liposome-based system. Therefore, multiple introduction of adjuvant molecules is suitable to prepare antigen carriers with high immunity-inducing effects for

effective cancer immunotherapy.

Acknowledgments

This work was supported by Grants-in-aid for Scientific Research from the Ministry of Education, Science, Sports, and Culture in Japan (15H03024, 26242049). Y. Yoshizaki thanks the research fellowship of Japan Society for the Promotion of Science (15J12180).

References

[1] C. Gedye, A. van der Westhuizen, T. John, Checkpoint immunotherapy for cancer: superior survival, unaccustomed toxicities, Intern. Med. J. 45 (2015) 696-701.

[2] S. A. Rosenberg, N. P. Restifo, Adoptive cell transfer as personalized immunotherapy for human cancer, Science 348 (2015) 62-68.

[3] J. Wang, E. L. Reinherz, Structural basis of cell–cell interactions in the immune system, Curr. Opin. Struct. Biol. 10 (2000) 656-661.

[4] M. P. Stewart, A. Sharei, X. Ding, G. Sahay, R. Langer, K. F. Jensen, *In vitro* and *ex vivo* strategies for intracellular delivery, Nature 538 (2016) 183-192.

[5] V. Dudu, V. Rotari, M. Vazquez, Sendai virus-based liposomes enable targeted cytosolic delivery of nanoparticles in brain tumor-derived cells, J Nanobiotechnology 10 (2012) 1-9.

[6] R. A. Schwendener, Liposomes as vaccie delivery systems: a review of the recent advances, Ther. Adv. Vaccines 2 (2014) 159-182.

[7] L. Bungener, K. Serre, L. Bijl, L. Leserman, J. Wilschut, T. Daemen, P. Machy, Virosome-mediated delivery of protein antigens to dendritic cells, Vaccine 20 (2002) 2287-2295.

[8] E. Yuba, A. Harada, Y. Sakanishi, K. Kono, Carboxylated hyperbranched poly(glycidol)s for preparation of pH-sensitive liposomes, J. Control. Release 149 (2011) 72-80.

[9] E. Yuba, A. Harada, Y. Sakanishi, S. Watarai, K. Kono, A liposome-based antigen delivery system using pH-sensitive fusogenic polymers for cancer immunotherapy, **Biomaterials 34 (2013)** 3042-3052.

[10] Y. Yoshizaki, E. Yuba, T. Komatsu, K. Udaka, A. Harada, K. Kono, Improvement of peptide-based tumor immunotherapy using pH-sensitive fusogenic polymer-modified liposomes, Molecules 21 (2016) 1284.

[11] E. Yuba, N. Tajima, Y. Yoshizaki, A. Harada, H. Hayashi, K. Kono, Dextran derivative-based pH-sensitive liposomes for cancer immunotherapy, Biomaterials 35 (2014) 3091-3101.

[12] E. Yuba, Y. Kanda, Y. Yoshizaki, R. Teranishi, A. Harada, K. Sugiura, T. Izawa, J. Yamate, N. Sakaguchi, K. Koiwai, K. Kono, pH-Sensitive polymer-liposome-based antigen delivery systems potentiated with interferon-γ gene lipoplex for efficient cancer immunotherapy, Biomaterials 67 (2015) 214-224.

[13] R. J. Greenwald, G. J. Freeman, A.H. Sharpe, The B7 family revisited, Annu. Rev. Immunol. 23 (2005) 515-548.

[14] J. Valenzuela, C. Schmidt, M. Mescher, The roles of IL-12 in providing a third signal for clonal expansion of naive CD8 T cells, J. Immunol. 169 (2002) 6842-6849.

[15] R. H. Schwartz, T cell anergy, Annu. Rev. Immunol. 21 (2003) 305-334.

[16] S. J. Szabo, B. M. Sullivan, S. L. Peng, L. H. Glimcher, Molecular mechanisms regulating Th1 immune responses, Annu. Rev. Immunol. 21 (2003) 713-758.

[17] A. Gardner, B. Ruffell, Dendritic cells and cancer immunity, Trends. Immunol. 37 (2016) 855-865.

[18] F. R. Vogel, Improving vaccine performance with adjuvants, Clin. Infect. Dis. 30 (2000) 266-270.

[19] E. B. Lindblad, Alumium compounds for use in vaccines, Immunol. Cell. Biol. 82 (2004) 497-505.

[20] C. Farace, P. Sánchez-Moreno, M. Orecchioni, R. Manetti, F. Sgarrella, Y. Asara, J. M. Peula-García, J. A. Marchal, R. Madeddu, L. G. Delogu, Immune cell impact of three differently coated lipid nanocapsules: pluronic, chitosan and polyethylene glycol, Sci. Rep. 6 (2016) 18423.

[21] M. Orecchioni, C. Ménard-Moyon, L. G. Delogu, A. Biancob, Graphene and the immune system: Challenges and potentiality, Adv. Drug Deliv. Rev. 105 (2016) 163–175.

[22] Y. Zhang, H. Pan, P. Zhang, N. Gao, Y. Lin, Z. Luo, P. Li, C. Wang, L. Liu, D. Pang, L. Cai, Y. Ma, Functionalized quantum dots induce proinflammatory responses in vitro: the role of terminal functional groupassociated endocytic pathways, Nanoscale 5 (2013) 5919.

[23] W. Yan, W. Chen, L. Huang, Mechanism of adjuvat activity of cationic liposome: Phosphorylation of a MAP kinase, ERK and induction of chemokines, Mol. Immunol. 44 (2007) 3672-3681.

[24] C. Lonez, M. Vandenbranden, J. M. Ruysschaert, Cationic lipids activate intracellular signaling pathways, Adv. Drug. Deliv. Rev. 64 (2012) 1749-1758.

[25] Y. Yoshizaki, E. Yuba, N. Sakaguchi, K. Koiwai, A. Harada, K. Kono, Potentiation of pH-sensitive polymer-modified liposomes with cationic lipid inclusion as antigen delivery carriers for cancer immunotherapy, Biomaterials 35 (2014) 8186-8196.

[26] T. Kawai, S. Akira, The role of pattern-recognition receptors in innate immunity: update on Toll-like receptors, Nat. Immunol. 11 (2010) 373-384.

[27] A. Stano, E. A. Scott, K. Y. Dane, M. A. Swartz, J. A. Hubbell, Tunable T cell immunity towards a protein antigen using polymersomes vs. solid-core nanoparticles, Biomaterials 34 (2013) 4339-4346.

[28] S. N. Thomas, E. Vokali, A. W. Lund, J. A. Hubbell, M. A. Swartz, Targeting the

tumor-draining lymph node with adjuvanted nanoparticles reshapes the anti-tumor immune response, Biomaterials 35 (2014) 814-824.

[29] Q. Liu, L. Jia, T. Yang, Q. Fan, L. Wang, G. Ma, Pathogen-mimicking polymeric nanoparticles based on dopamine polymerization as vaccines adjuvants induce robust humoral and cellular immune responses Small 12 (2016) 1744-1757.

[30] P. C. B. de Faria, L. I. dos Santos, J. P. Coelho, H. B. Ribeiro, M. A. Pimenta, L. O. Ladeira, D. A. Gomes, C. A. Furtado, R. T. Gazzinelli, Oxidized multiwalled carbon nanotubes as antigen delivery system to promote superior CD8+ T cell response and protection against cancer, Nano Lett. 14 (2014) 5458-5470.

[31] C. Bode, G. Zhao, F. Steinhagen, T. Kinjo, D. M. Klinman, CpG DNA as a vaccine adjuvant, Expert. Rev. Vaccines 10 (2011) 499-511.

[32] M. Mansourian, A. Badiee, S. A. Jalali, S. Shariat, M. Yazdani, M. Amin, M. R. Jaafari, Effective induction of anti-tumor immunity using p5 HER-2/neu derived peptide encapsulated in fusogenic DOTAP cationic liposomes co-administerated with CpG-ODN, Immunol. Lett. 162 (2014) 87-93.

[33] Z. Shen, G. Reznikoff, G Dranoff, KL. Rock, Cloned dendritic cells can present exogenous antigens on both MHC class I and class Ⅱ molecules, J. Immunol. 158 (1997) 2723-2730.

[34] M. W. Moore, F. R. Carbone, M. J. Bevan, Introduction of soluble protein into the class I pathway of antigen processing and presentation, Cell 54 (1988) 777-785.

[35] J. Canton, D. Neculai, S. Grinstein, Scavenger receptors in homeostasis and immunity, Nat. Rev. Immunol. 13 (2013) 621-634.

[36] L. Peiser, S. Mukhopadhyay, S. Gordon, Scavenger receptors in innate immunity, Curr. Opin. Immunol. 14 (2002) 123-128.

[37] G. Trinchieri, Interleukin-12 and the regulation of innate resistance and adaptive immunity, Nat. Rev. Immunol. 3 (2003) 133-146.

[38] D. A. Muruve, V. Petrilli, A. K. Zaiss, L. R. White, S. A. Clark, P. J. Ross, R. J. Parks, J. Tschopp, The inflammasome recognizes cytosolic microbial and host DNA ad triggers an innate immune response, Nature 452 (2008) 103-107.

Table 1. Particle size and ζ-potential of liposomes

Liposome	Mean diameter (nm)	ζ-potential (mV)
Lip	97 ± 6	- 18 ± 6
Pre-mix (TRX–)	100 ± 3	- 19 ± 5
Post-mix (TRX–)	88 ± 6	-11 ± 1
TRX-Lip	110 ± 6	- 63 ± 4
Pre-mix (TRX+)	108 ± 8	- 65 ± 3
Post-mix (TRX+)	109 ± 10	- 60 ± 5

Figure captions

Figure 1. Design of pH-sensitive polymer (MGlu-HPG)-modified liposomes based immunity-inducing system containing cationic lipid (TRX) and Toll-like receptor 9 ligand (CpG-DNA) for efficient antigen delivery and activation of dendritic cells. These liposomes deliver not only double stimulation molecules, CpG-DNA and cationic lipids, to endosomes but also antigen to cytosol of dendritic cells after endosomal membrane destabilization by MGlu-HPG. Antigen in cytosol is presented to T lymphocytes through MHC class Ⅰ molecule and up-regulation of co-stimulatory molecules and cytokine production by double stimulation molecules promote the activation of cytotoxic T lymphocytes.

Figure 2. Preparation schemes of antigen-loaded liposomes used in this study.

Figure 3. The amounts of CpG-DNA in Pre-mix liposomes with (closed symbols) or without (open symbols) TRX at various feeds of CpG-DNA. ** $p < 0.01$.

Figure 4. (A) Relative fluorescence intensity of DC2.4 cells treated with 0.6 mol% Rh-PE-labeled liposome. Cells were incubated with liposomes for 4 h at 0.5 mM of lipids and 2.5 μg/mL of CpG-DNA in the absence of serum. (B) Relative fluorescence intensity of DC2.4 cells treated with FITC-CpG-DNA-complexed liposome. Cells were incubated with liposomes for 4 h at 0.1 mM of lipids and 0.5 μg/mL of FITC-CpG-DNA

in the absence of serum. * $p < 0.05$. ** $p < 0.01$.

Figure 5. (A) CLSM images of DC2.4 treated with FITC-CpG-DNA or various liposomes. Cells were incubated with 0.6 mol% Rh-PE-labeled liposomes for 4 h at 0.1 mM of lipids and 0.5 μg/mL of FITC-CpG-DNA in the absence of serum. Scale bar represents 10 μm. (B) Co-localization analysis of FITC fluorescence with rhodamine fluorescence in region of interest (ROI) indicated with white dashed-lines in Figure 5A. (C) CLSM images of DC2.4 cells treated with Pre-mix TRX+ containing Rh-PE (left) or FITC-CpG-DNA (right). Cells were stained by LysoTracker Green (left) or Red (right). (D) Co-localization analysis of fluorescence derived from endo/lysosomes with fluorescence derived from liposomes or CpG-DNA in ROI indicated with white dashed-lines in Figure 5C.

Figure 6. TNF-α (A) and IL-12 (B) productions from DC2.4 cells treated with liposomes for 24 h in the absence of serum. Lipid and CpG-DNA concentrations were 0.5 mM and 2.5 μg/mL, respectively. After incubation, each cell medium was collected and centrifuged, and then cytokine levels in the supernatant were measured by ELISA. * $p < 0.05$. ** $p < 0.01$.

Figure 7. Immunofluorescent staining of DC2.4 treated with CpG-DNA or various liposomes. Cells were incubated with liposomes for 6 h at 0.1 mM of lipid

concentration and 0.5 μg/mL of CpG-DNA concentration in the absence of serum. Then cells were incubated with cell culture medium containing 10% FBS for 20 h. After incubation, surface molecules of cells were stained using specific antibodies. * $p < 0.05$.

Figure 8. *In vitro* stimulation of splenocytes from mice immunized with 50 μg OVA-loaded and 0 or 1 μg CpG-DNA-complexed liposomes at days 7 and 14. 7 days after second immunization, splenocytes (4×10^6/2 mL) isolated from immunized C57BL/6 mice were incubated with or without 50 μg/mL, 25 μg/mL of OVA for 5 days. IFN-γ production in the supernatant was measured by ELISA. * $p < 0.05$. ** $p < 0.01$.

Figure 9. (A-D) Antitumor effects induced by subcutaneous administration with OVA-loaded various liposomes. C57BL/6 mice were immunized on days 5 and 12 with PBS (closed diamonds), TRX-Lip (closed circles), Pre-mix TRX– (open triangles), Pre-mix TRX+ (closed triangles), Post-mix TRX+ (closed squares), TRX-Lip and CpG-DNA injected different sites (closed diamonds). Arrows indicated the days of sample administration. Changes in tumor volume of mice (A, C) were monitored after E.G7-OVA cells (1×10^6 cells/mouse) inoculation. All treated groups contained four mice. The amounts of OVA and CpG-DNA administered were 50 μg and 1 μg per mouse, respectively. (B, D) Kaplan-Meier curves for (A) and (C), respectively. (E, F) Antitumor effects for late stage tumor induced by subcutaneous administration with

OVA-loaded various liposomes. C57BL/6 mice were immunized on days 9 and day 16 with PBS (open diamonds), Lip (open circles), TRX-Lip (closed circles), Post-mix TRX+ (closed squares). Change in tumor volume of mice (E) was observed after E.G7-OVA cells (1×10^6 cells/mouse) inoculation. (F) Kaplan-Meier curves for (E).

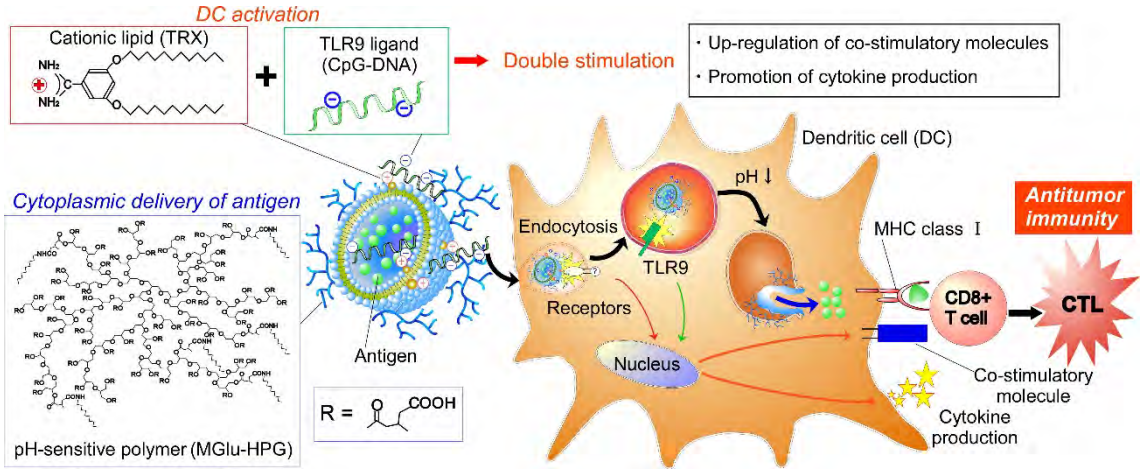

Figure 1.

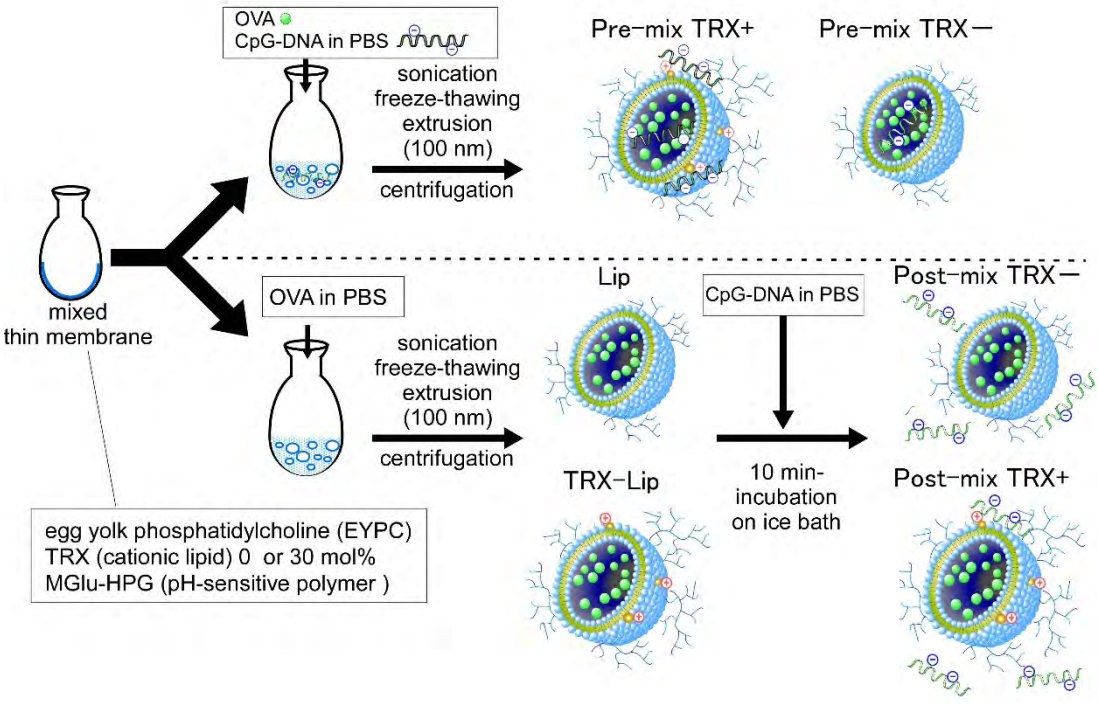

Figure 2.

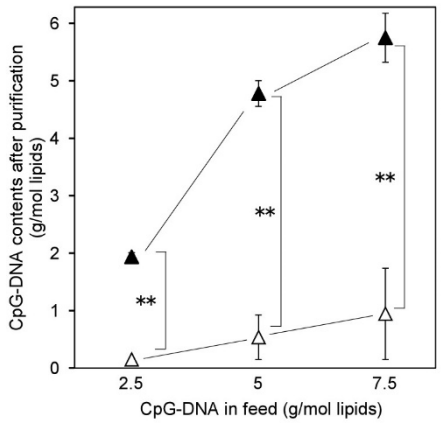

Figure 3.

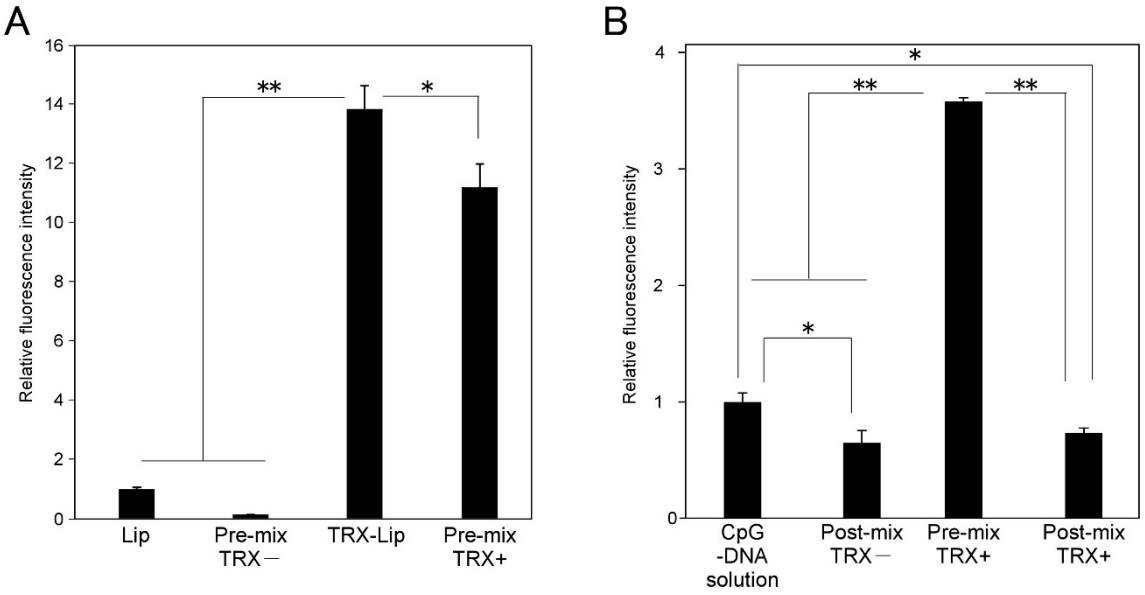

Figure 4.

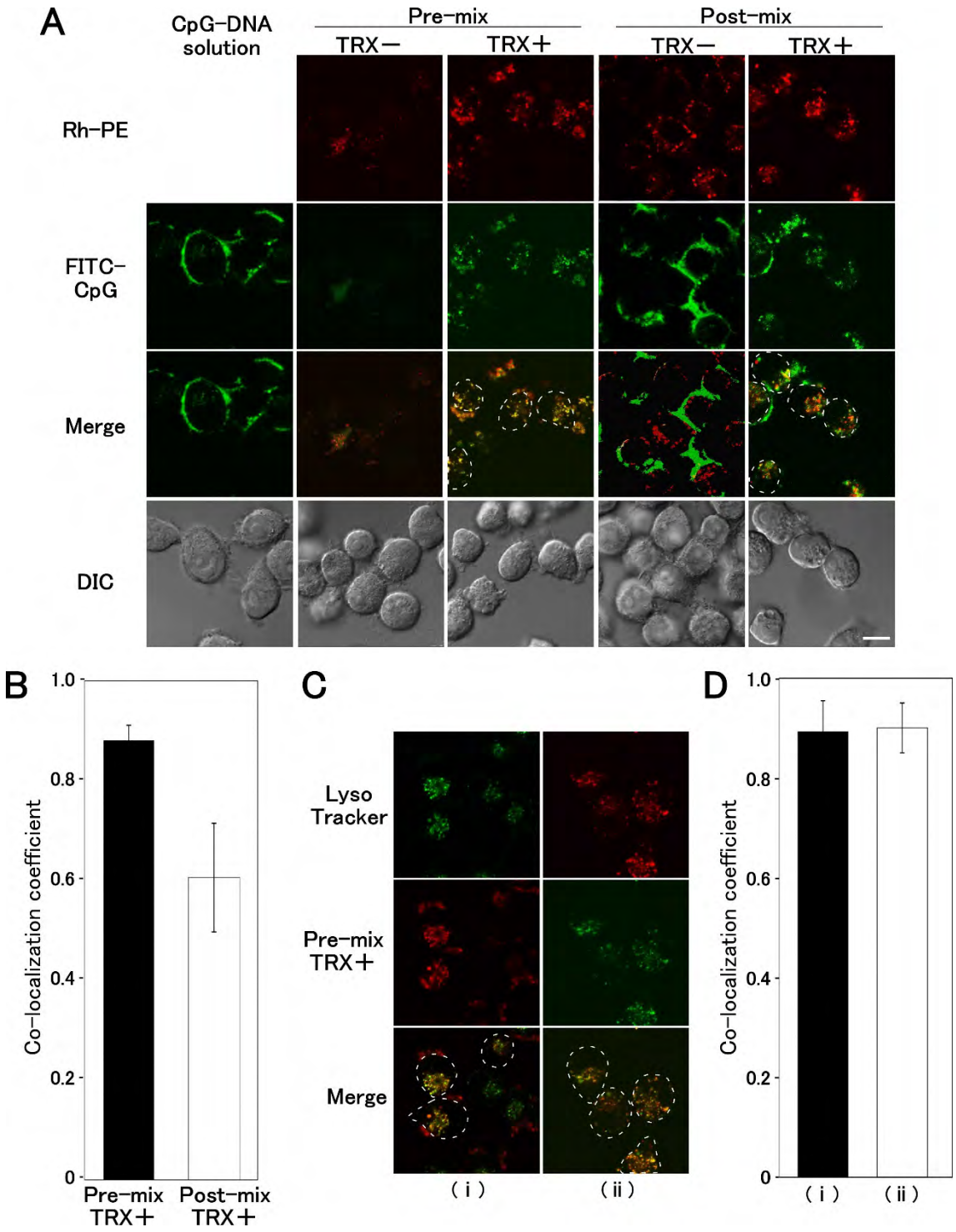
A
CpG-DNA solution
Pre-mix
Post-mix
TRX−
TRX+
TRX−
TRX+
Rh-PE
FITC-CpG
Merge
DIC
B
Co-localization coefficient
1.0
0.8
0.6
0.4
0.2
0
Pre-mix TRX+
Post-mix TRX+
C
Lyso Tracker
Pre-mix TRX+
Merge
(i)
(ii)
D
Co-localization coefficient
1.0
0.8
0.6
0.4
0.2
0
(i)
(ii)

Figure 5.

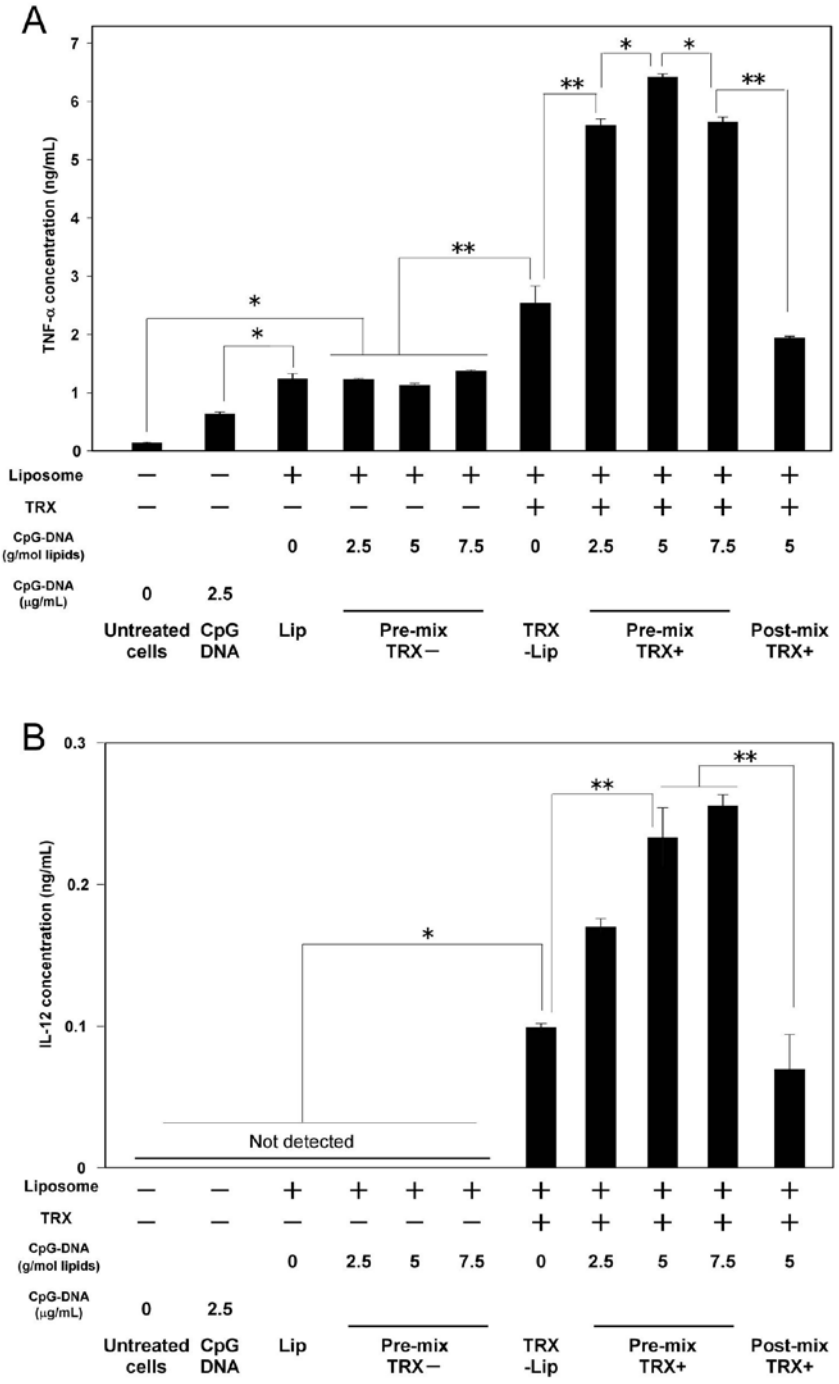
A
TNF-α concentration (ng/mL)
Liposome
TRX
CpG-DNA (g/mol lipids)
CpG-DNA (μg/mL)
Untreated cells
CpG DNA
Lip
Pre-mix TRX−
TRX -Lip
Pre-mix TRX+
Post-mix TRX+
B
IL-12 concentration (ng/mL)
Not detected
Liposome
TRX
CpG-DNA (g/mol lipids)
CpG-DNA (μg/mL)
Untreated cells
CpG DNA
Lip
Pre-mix TRX−
TRX -Lip
Pre-mix TRX+
Post-mix TRX+

Figure 6.

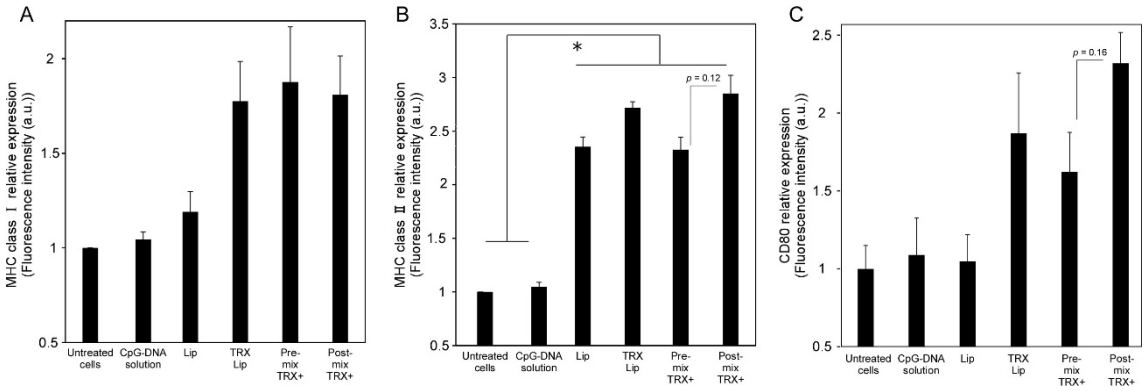

Figure 7.

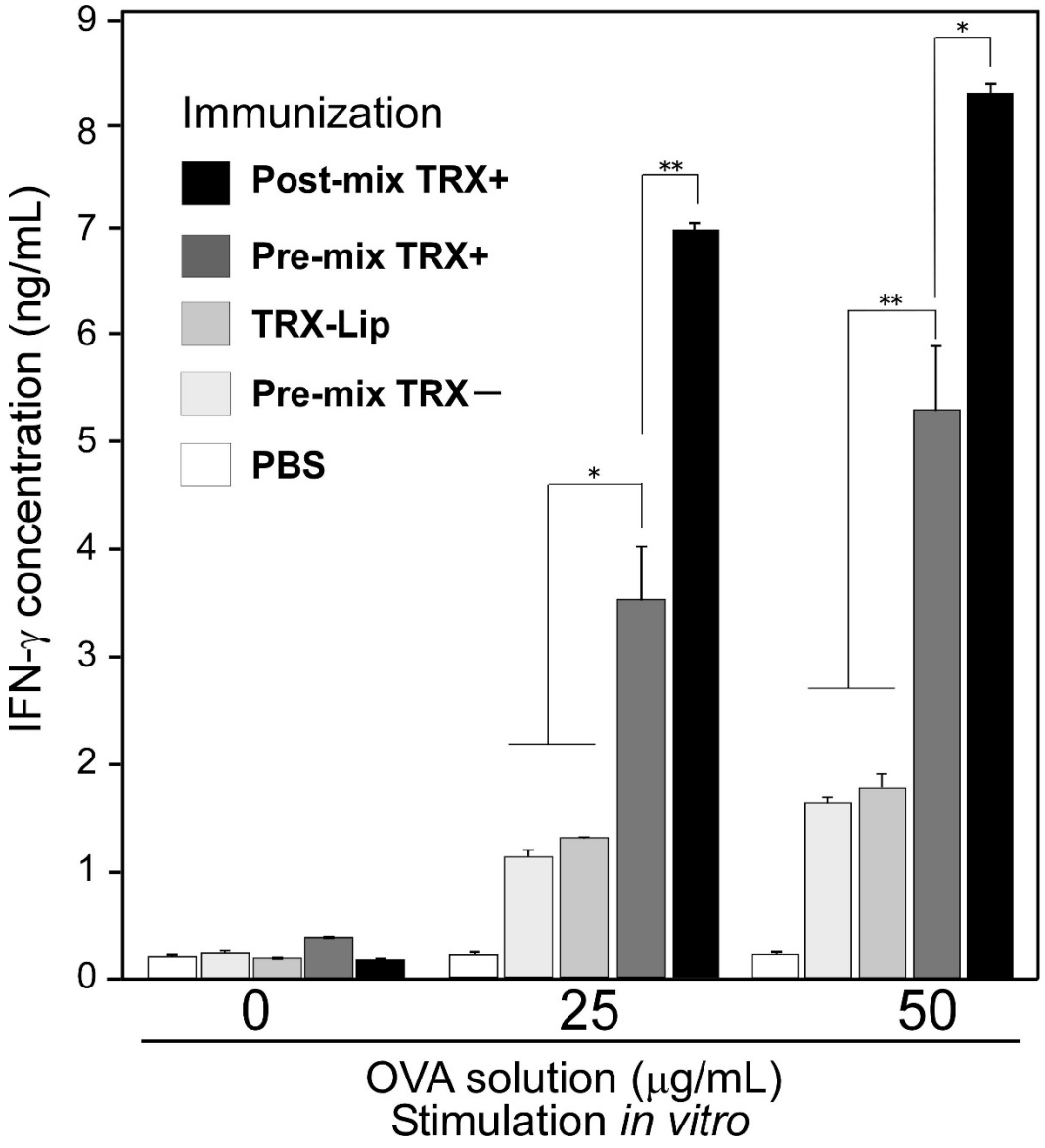

Figure 8.

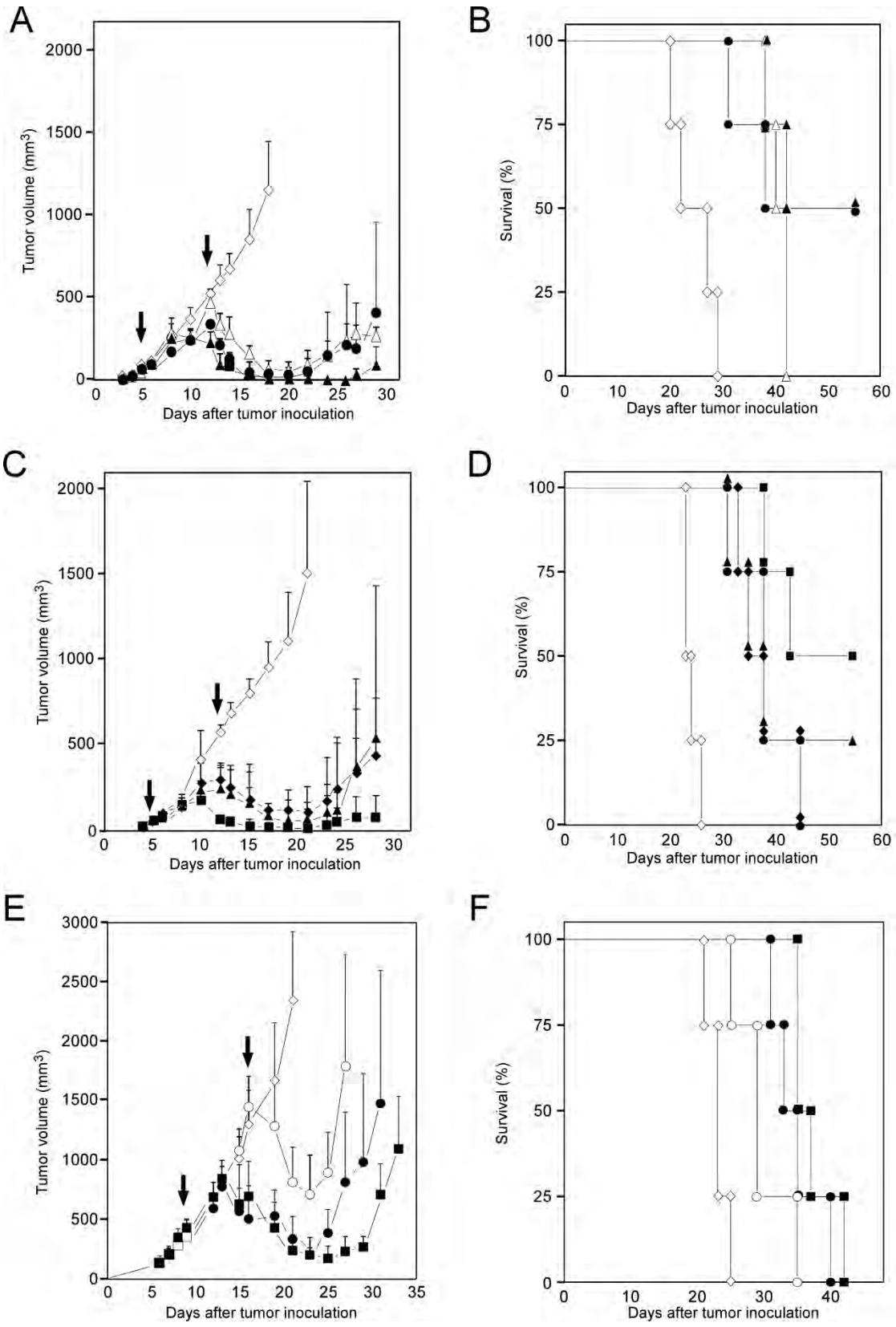
A
Tumor volume (mm3)
Days after tumor inoculation
B
Survival (%)
Days after tumor inoculation
C
Tumor volume (mm3)
Days after tumor inoculation
D
Survival (%)
Days after tumor inoculation
E
Tumor volume (mm3)
Days after tumor inoculation
F
Survival (%)
Days after tumor inoculation

Figure 9.